In situ investigations of bimetallic potassium erbium borohydride

Michael Heere[a], SeyedHosein Payandeh GharibDoust[b], Magnus H. Sørby[a], Christoph Frommen[a], Torben R. Jensen[b] and Bjørn C. Hauback[a]

[a] Physics Department, Institute for Energy Technology, NO-2027 Kjeller, Norway

[b] Interdisciplinary Nanoscience Center (iNANO) and Department of Chemistry, University of Århus, Langelandsgade 140, DK-8000 Århus C, Denmark

Keywords: borohydride, rare earth, hydrogen storage, decomposition, *in situ* XRD

Abstract

Research on rare earth (RE) borohydrides is increasing due to their potential as possible hydrogen storage materials and as solid-state Li-ion conductors for battery applications. In this work, we report the formation of a new bimetallic RE borohydride, $KEr(BH_4)_4$, via mechanochemical reaction between KBH_4 and $Er(BH_4)_3$ in a molar ratio of 1:1. Post-annealing of the ball-milled mixture at 175 °C for 12 h under 40 bar of hydrogen resulted in an almost phase pure material. $KEr(BH_4)_4$ is isostructural to $NaSc(BH_4)_4$ with lattice parameters of a = 8.4472(8) Å, b = 12.4292(11) Å, c = 9.6252(9) Å and space group *Cmcm*. An amorphization of the new bimetallic phase was observed at ~170 °C under 1 bar argon via temperature programmed photographic analysis, which is in agreement with *in situ* synchrotron radiation powder X-ray diffraction (SR-PXD) as well as thermogravimetric and differential scanning calorimetry (TG-DSC). The *in situ* SR-PXD data did not show decomposition into the starting monometallic borohydrides.

Introduction

Metal hydrides are used in technological applications, where the largest commercial success has been the nickel-metal hydride battery (Ni-MH), with over 1 billion cells sold in 2015 [1]. In Ni-MH batteries, rare earth based metal hydrides related to $LaNi_5H_x$, are employed for the anode [2, 3]. Complex metal hydrides based on rare earth metals and boron also show great potential [4, 5], for example rare earth (RE) borohydrides have received an increasing amount of interest as solid state hydrogen storage materials [6-26], solid state electrolytes [27-31], luminescent [32] and magnetocaloric materials [33, 34] during the past 10 years, and many new compounds and crystal structures of RE based hydrides have been extensively studied [35].

RE borohydrides show a big variety of crystal structures and can be categorized as follows. The early lanthanides La, Ce, Pr and Nd form $LiRE(BH_4)_3Cl$ complexes in space group *I*-43*m* [11, 19]. The $RE(BH_4)_3$ with RE = La, Ce crystallize in *R*-3*c* [36], respectively. Pr, Nd, Sm, Gd, Tb, Er, and Yb form α-$RE(BH_4)_3$ (*Pa*-3) with a polymorphic phase transition to β-$RE(BH_4)_3$ for Y, Er, Yb (*Pm*-3*m*/*Fm*-3*m*) [8, 10, 12, 19, 23]. The smallest lanthanides Yb and Lu form $[RE(BH_4)_4]^-$ complex anions which are stabilized by Li^+ cations (space group *P*-42*c*), and they are in analogy to $MSc(BH_4)_4$ (M = Li, Na, K) [7, 21, 37, 38]. Trivalent borohydrides with Sm and Eu are reduced to $RE(BH_4)_2$ upon heating, which are isostructural to $Sr(BH_4)_2$ (*Pbcn*) [20]. Recently the bimetallic $NaLa(BH_4)_4$ and $K_3La(BH_4)_6$ with space groups *Pbcn* and $P2_1/n$, respectively, have been reported [39].

In this study, we report on the synthesis and thermal properties of a new bimetallic borohydride, $KEr(BH_4)_4$. This compound was obtained through a combination of mechanochemical synthesis followed by thermal treatment. Simultaneous thermogravimetric (TG) and differential scanning calorimetry (DSC) in combination with *in situ* SR-PXD have been used to elucidate the decomposition pathway in order to determine reaction products and intermediates.

Experimental

KBH_4 (95%), $ErCl_3$ (99.9%), $LiBH_4$ (95%) and dimethyl sulfide (DMS, anhydrous, 99.9%) were purchased from Sigma Aldrich. All sample preparation and synthesis of $Er(BH_4)_3$ were carried out according to the procedures described in Ref. [23].

$Er(BH_4)_3$ and KBH_4 were ball milled in a molar ratio of 1:1 and post annealed at 175 °C for 12 h under 40 bar of hydrogen in a Sieverts type apparatus [40]. Ball milling was carried out using a Fritsch Pulverisette 6 planetary mill with an 80 ml tungsten carbide coated steel vial and balls. A ball to powder ratio of 40:1 and milling times of 1 h (4x15 min with 5 min breaks) were employed. All sample handling was executed under inert conditions with O_2 and H_2O levels kept below 1 ppm, in an MBraun glove box.

Powder X-ray Diffraction (PXD) data were collected using a Bruker AXS D8 Advance. The data were collected in transmission mode with CuKα λ=1.5418 Å, a Göbel mirror and a LynxEye™ 1D strip detector. The samples were contained in 0.5 mm sealed boron glass capillaries.

In situ SR-PXD data were collected at the Swiss Norwegian Beam Line (SNBL), BM01A at the European Synchrotron Radiation Facility (ESRF), Grenoble, France. Sapphire capillaries with 1.2 mm and 0.8 mm outer and inner diameter were connected to an in-house manufactured remote controlled gas rig and high pressure manifold cell. The sample-to-detector distances were 146 and

345.8 mm, respectively, and the wavelength was 0.77787 Å, calibrated from a NIST LaB_6 standard. Data were collected using a Pilatus 2M detector. The exposure time was set to 30 s giving a temperature resolution of 2.5 °C/pattern and the sapphire capillary was rotated by 10° during exposure to improve powder averaging. Single crystal reflections from the sapphire tube were masked manually in Fit2D and Bubble [41, 42]. Rietveld refinements were performed using GSAS and Expgui software [43, 44]. The Bragg peak profiles were modelled with a Thompson-Cox-Hastings pseudo-Voigt function with three Gaussian and one Lorentzian parameter [45]. The background was fitted with a shifted Chebyshev polynomial with up to 36 terms. Atomic positions for $KEr(BH_4)_4$ and KBH_4 were taken from Ref. [37, 46, 47]. The crystal structure of $KEr(BH_4)_4$ was refined with the data shown in Fig. 3 at room temperature (RT). BH_4 units were treated as rigid bodies with B-H distances of 1.13 Å.

Simultaneous thermogravimetric and differential scanning calorimetry (TG-DSC) experiments were conducted using a Netzsch STA 449 F3 Jupiter analyzer. The samples were loaded in Al pans (~5 – 10 mg) and heated from RT to 400 °C at a heating rate of 5 °C min^{-1}. Furthermore, the annealed sample was heated from RT to 200 °C and cooled down to 60 °C at a rate of 5 °C min^{-1}. The Ar purge gas rate was set to 50 ml min^{-1} and the protection gas flow to 20 ml min^{-1}.

Temperature programmed desorption (TPD-MS) was performed in an in-house manufactured apparatus connected to a MKS Microvision-IP Residual Gas Analyser. The powder was loaded in a steel sample holder (~10 mg) and heated from RT to 400 °C with a heating rate of 5 °C min^{-1} under dynamic vacuum.

Temperature programmed photographic analysis (TPPA) was conducted on the ball milled sample. Approximately 30mg of the powder was pressed using a pressing die and a pellet with diameter of 6 mm was prepared. The pallet was transferred to a glass tube and sealed under argon. The glass tube was placed in a home-built aluminum heating block as described in [48] and a camera was placed in front of the sample. Sample was heated from RT to 500 °C with a heating rate of 5°C /min, while photos of the sample were collected every 5 s.

Results and Discussion

a) $Er(BH_4)_3 + KBH_4$ as milled

Fig. 1a shows *in situ* SR-PXD data of the as milled $Er(BH_4)_3 + KBH_4$ from RT to 600 °C, whereas Fig. 1b presents the SR-PXD data at selected temperatures between RT and 600 °C for a better visualization. Only Bragg peaks of two phases $Er(BH_4)_3$ and KBH_4 are present at RT. Upon heating, at 97 °C the

Bragg peaks of $KEr(BH_4)_4$ (two Bragg peaks shown by black arrows in Fig. 1a) are increasing in intensity and reach their strongest intensity at 168 °C (blue curve) while peak intensities for the reactants $Er(BH_4)_3$ and KBH_4 are decreasing. The Bragg peaks for the bimetallic phase resembles those of $NaSc(BH_4)_4$ and $KHo(BH_4)_4$ [37, 46], thus indicating an isostructural relationship. The Bragg reflections of $KEr(BH_4)_4$ decrease rapidly from 168 °C and disappear at 176 °C (magenta curve) with diffuse scattering appearing. Simultaneously, peak intensities for KBH_4 and $Er(BH_4)_3$ are rapidly decreasing.

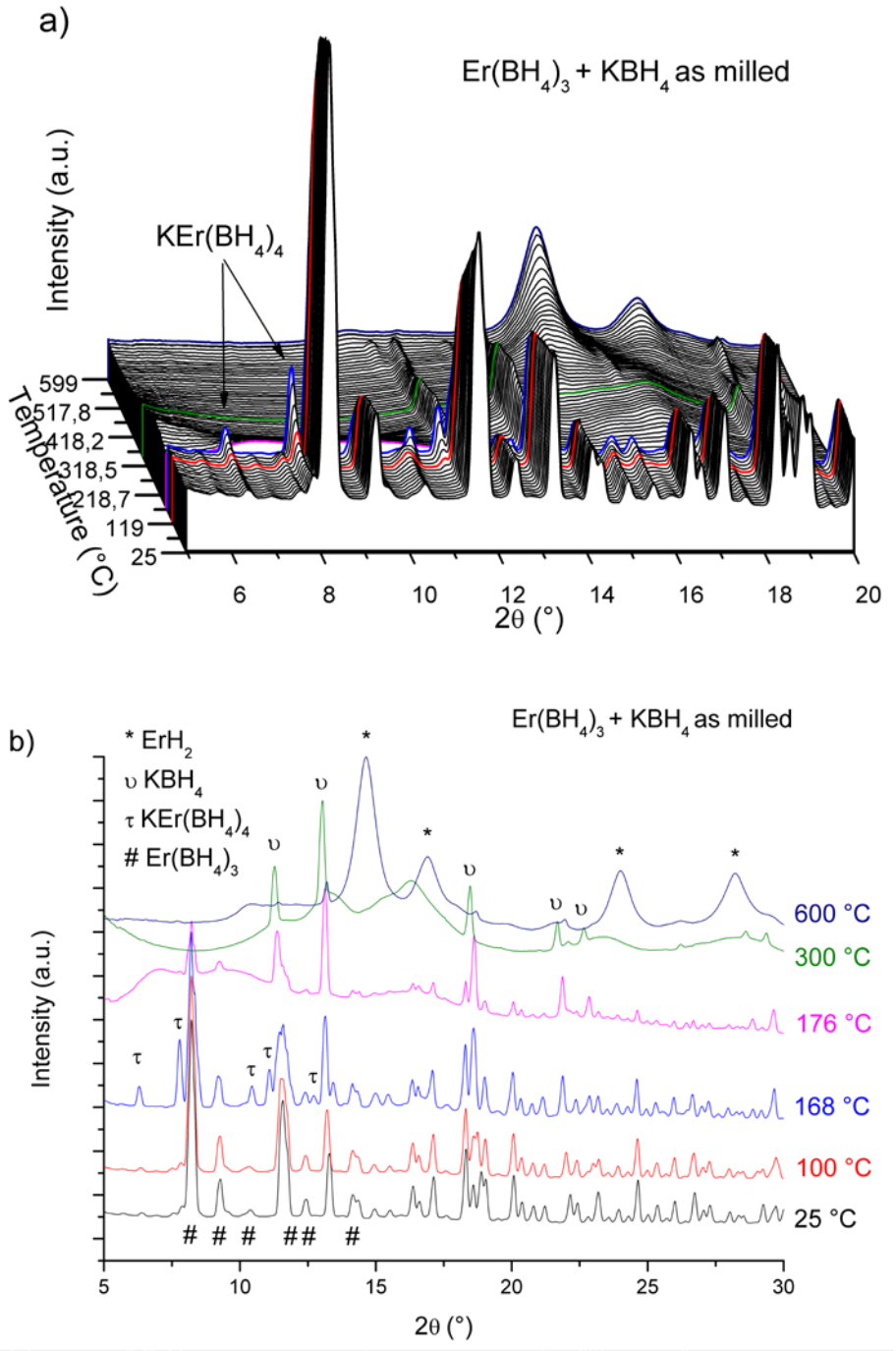

Fig. 1 a) *In situ* SR-PXD data of ball milled $Er(BH_4)_3$ + KBH_4 heated from RT to 600 °C under 1 bar H_2 (temperature ramp of 5 °C min^{-1}). b) SR-PXD data at specific temperatures. Curves in color are shown from a) for better visualization. λ = 0.77787 Å.

Once the Bragg reflections of $KEr(BH_4)_4$ have disappeared, peak intensities for KBH_4 remain stable, whereas peak intensities for $Er(BH_4)_3$ continue to decrease and are no longer detected at 260 °C. This shows that $Er(BH_4)_3$ is decomposed. Between 300 and 600 °C the diffuse scattering decreases and Bragg peaks of ErH_2 appear (green and dark blue curve in Fig. 1). From 572 to 600 °C peak intensities for KBH_4 are decreasing, which is in agreement with the reported decomposition temperature for KBH_4 of 584 °C [49]. However, traces of KBH_4 remains visible during the timeframe of the measurement.

TPPA was performed on a pressed pellet of ball-milled mixture of $Er(BH_4)_3$ + KBH_4 to investigate whether the disappearance of Bragg peaks form $KEr(BH_4)_4$ around 170 °C was due to melting. The pellet shows a color change around 176 - 183 °C corresponding to the formation of $KEr(BH_4)_4$. However, no melting was observed and the sample was decomposed upon further heating to 500 °C, thus showing that the loss of crystallinity is due to a solid-state amorphization. Selected TPPA pictures are shown in the supplementary information (Fig. A2).

The combined TG-DSC data for the as milled mixture of $Er(BH_4)_3$ and KBH_4 are presented in Fig. 2a. In the DSC trace a first endothermic event is observed with a peak temperature of 170 °C. This is in good agreement with *in situ* SR-PXD data where loss of crystallinity is observed around 176 °C. The nature of this amorphization is not settled. However, the Bragg peaks from $Er(BH_4)_3$ and KBH_4 in the SR-PXD data do not increase when the Bragg peaks of the bimetallic phase disappear, thus showing that $KEr(BH_4)_4$ does not phase-separates into crystalline KBH_4 and $Er(BH_4)_3$. A mass loss of 1 wt% is observed at the same temperature, which is believed to be due to loss of remaining solvent in the reactants.

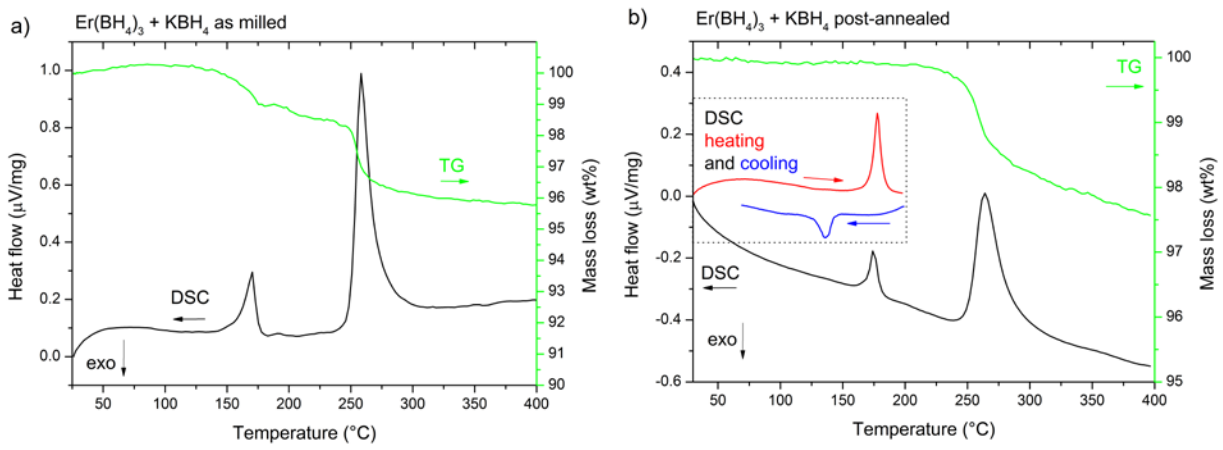

Fig. 2 a) TG-DSC data of as milled $Er(BH_4)_3$+KBH_4 from RT to 400 °C; b) TG-DSC data of post-annealed $Er(BH_4)_3$+KBH_4: heating from RT to 200 °C and cooling from 200 to 60 °C (dashed box in top left corner). Black curves show a second heating of the same sample from RT to 400 °C.

From DSC data the major decomposition event of $Er(BH_4)_3$ is found to be endothermic [23] at an onset and peak temperature of 250 and 258 °C, respectively. This is in good agreement with the disappearance of Bragg peaks of $Er(BH_4)_3$ in the SR-PXD data and within ~5 °C of that reported for decomposition temperature of pure $Er(BH_4)_3$ [23]. It is not clear, yet, at which temperature the amorphous bimetallic compound is completely decomposed, but it is appears that its decomposition has no influence on decomposition temperature of $Er(BH_4)_3$. The theoretical weight loss for the decomposition of $Er(BH_4)_3$ to ErH_2 or ErH_3 accounts for 3.8 and 3.4 wt% H_2, respectively, which is in good agreement with the measured weight loss of 3.2 wt% (4.2 wt% in total).

b) $Er(BH_4)_3$ + KBH_4 post-annealed

In order to obtain a phase-pure bimetallic $KEr(BH_4)_4$, the ball milled mixture was heat treated for 12 h under 40 bar of hydrogen. An annealing temperature of 175 °C was chosen based on the initial assumption that the first DSC signal for the as-milled sample was due to the formation of the bimetallic phase. The TG data in Fig. 2a suggested that the first endothermic DSC signal was accompanied by a weight loss, and the 40 bar hydrogen pressure was employed to suppress the assumed partial decomposition. The post-annealed sample was analyzed by SR-PXD and Fig. 3 shows the RT data. Despite an annealing temperature above the amorphization temperature observed for the as-milled sample, the RT SR-PXD show a well-crystalline material with two different phases present: $KEr(BH_4)_4$ and KBH_4. This either means that the amorphization is reversible on cooling or that the applied hydrogen pressure increases the amorphization temperature. Annealing in vacuum or argon atmosphere have not been carried out, since the desired bimetallic phase was obtained in the first attempt. The lattice parameters for $KEr(BH_4)_4$ and KBH_4 are refined to a = 8.4472(8), b =

12.4292(11), c = 9.6252(9) Å and a = 6.745(17) Å, respectively. The phase fractions for $KEr(BH_4)_4$ and KBH_4 are determined to 97.5(3) and 2.5(3) wt%, thus indicating an almost complete reaction to the bimetallic compound. The atomic positions for $KEr(BH_4)_4$ have been refined (Table A1†) and agree within the standard deviations with those reported for the isostructural compounds $NaSc(BH_4)_4$ and $KHo(BH_4)_4$.

TG-DSC data of the post-annealed $Er(BH_4)_3$ and KBH_4 is shown in Fig. 2b. To clarify the origin of the first endothermic peak shown in Fig. 2a, two measurements have been conducted on the same sample. The first measurement shows heating from RT to 200 °C followed by cooling to 60 °C. The observed endothermic event at T_{peak}=177 °C reappears upon cooling as an exothermic peak at T_{peak}=136 °C. This shows that the reaction leading to amorphization is at least partly reversible. A weight loss of 0.4 wt% is observed as well (not shown), which is in good agreement with TPD-MS, showing the release of H_2 and minor amounts of other species (B_2H_6, $S(CH_3)_2$) (Fig. A2†). The second TG-DSC measurement presents the heating from RT to 400 °C with the same sample heated/cooled before. The DSC trace shows similarities to the as milled sample exhibits with two endothermic events between RT and 400 °C. The first one occurs at a peak temperature of 174 °C. The second event, which we attribute to the major decomposition of the material, has onset and peak temperatures of 250 and 264 °C, respectively (black curves in Fig. 2b). The mass loss is 2.5 wt% (Fig. 2b) and solely associated with the last event, thus supporting the assumption that the mass loss at lower temperature observed for the as-milled sample is due to loss of remnant solvent.

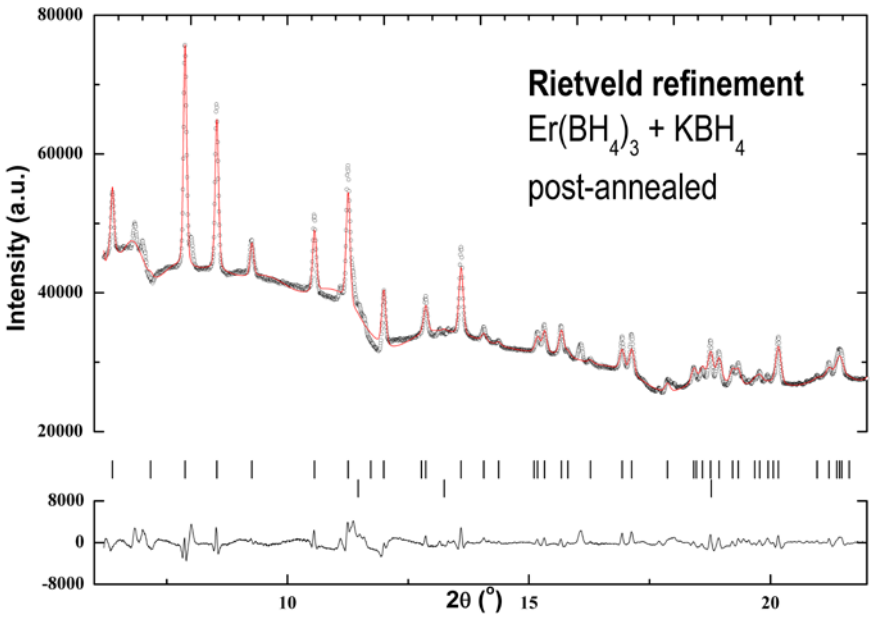

Fig. 3 Rietveld refinements with the SR-PXD data of post-annealed $Er(BH_4)_3$ + KBH_4 at RT showing experimental (circles) and calculated (red curve) patterns and a difference plot (below). Vertical ticks mark the

Bragg peak positions for $KEr(BH_4)_4$ and KBH_4 (from top). Fluctuations in the background result from the masking of single crystal sapphire peaks (sapphire tube). R_{wp} = 2.12%. λ = 0.77787 Å;

In situ SR-PXD data of the post-annealed $Er(BH_4)_3$ + KBH_4 (Fig. 4) have been collected between RT and 200 °C. All major Bragg peaks observed at RT can be assigned to $KEr(BH_4)_4$. The Rietveld fit to the RT data are shown in Fig. 3. The Bragg peaks of KBH_4 reappear from 50 °C, which is assumed to be a recrystallization effect. The bimetallic phase turns amorphous at 171 °C, which is in good agreement with the DSC data (177 °C). No Bragg peaks of $Er(BH_4)_3$ can be detected afterwards. Furthermore, the intensity of the KBH_4 peaks does not increase when the Bragg peaks of the bimetallic phase disappear, thus confirming that the $KEr(BH_4)_4$ does not phase separate back to crystalline KBH_4 and $Er(BH_4)_3$ at this temperature.

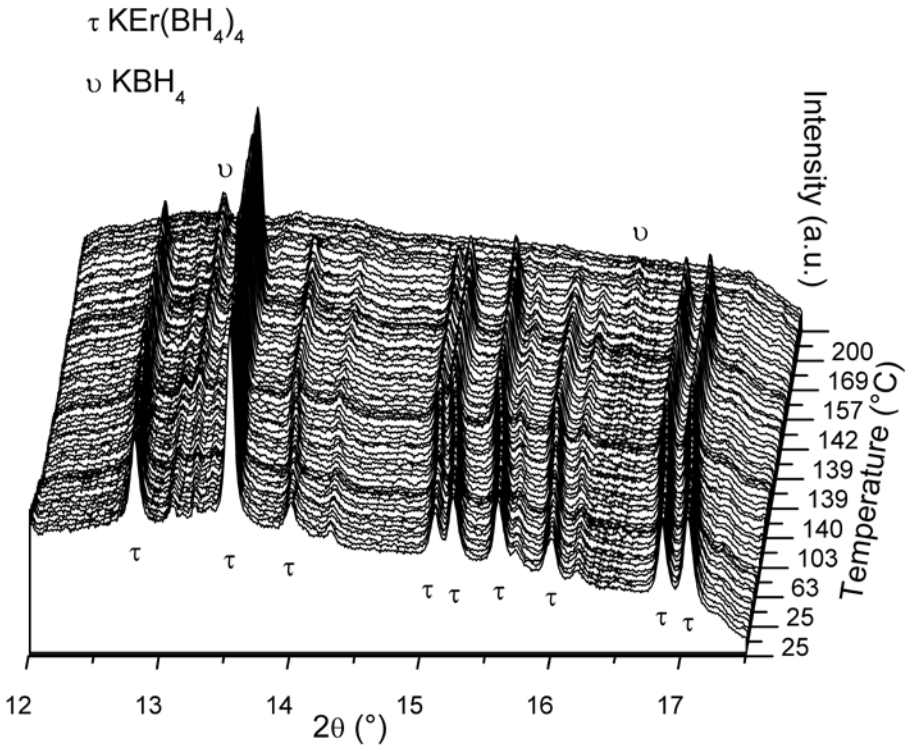

Fig. 4 *In situ* SR-PXD decomposition from post-annealed $Er(BH_4)_3$ + KBH_4 under 2 bar H_2. Data collected between RT and 200 °C with heating rates of 5 °C min^{-1} from RT to 140 °C and 170 to 200 °C. Between 140 and 170 °C the heating rate was reduced to 2 °C min^{-1}. Rietveld refinements with phase composition for initial state (front) are given in Fig. 3. λ = 0.77787 Å.

c) Decomposition under high hydrogen pressure

In situ SR-PXD decomposition experiment of the post-annealed sample was continued under a hydrogen pressure of 75 bar between 200 and 300 °C. Four different temperatures were chosen for isothermal treatment (marked in green in Fig. 5), 200, 220, 250 and 300 °C, which are all above the amorphization temperature of the post-annealed sample (Fig. 4). This served the purpose to promote the formation of crystalline decomposition products and intermediates. The sample was

kept isothermal under 75 bar of hydrogen for 22 min at each of these four temperatures and then heated with a rate of 5 °C min^{-1} between the isothermal steps. At 200 and 220 °C no reaction and no recrystallization occur. At 250 °C very weak Bragg peaks of ErH_3 (*P*-3*c*1) appear and increase in intensity. At 300 °C the Bragg peaks of ErH_3 and KBH_4 increase in intensity abruptly. We conclude for the post-annealed compound that the bimetallic phase decomposes between 250 and 300 °C, which is in good agreement with the decomposition from DSC data (T_{onset} = 250 °C), taking into account that the decomposition temperature should be higher under H_2 pressure. The formation of ErH_3 and KBH_4 is observed as decomposition products.

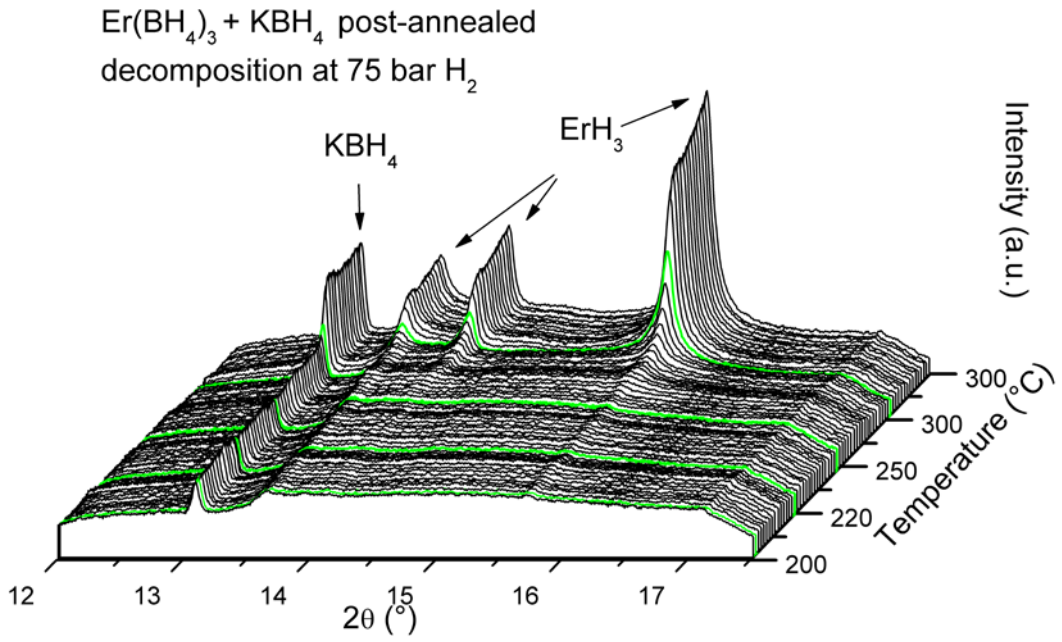

Fig. 5 *In situ* SR-PXD decomposition at high hydrogen pressure from post-annealed $Er(BH_4)_3$ + KBH_4. Data collected at 200, 220, 250 and 300 °C (green curves) under 75 bar H_2 (temperature ramp of 5 °C min^{-1}). λ = 0.77787 Å.

Conclusion

A new bimetallic RE-borohydride, $KEr(BH_4)_4$, was synthesized by ball milling of $Er(BH_4)_3$ and KBH_4 and post annealing at 175 °C for 12 h under 40 bar of hydrogen. The compound is isostructural to $NaSc(BH_4)_4$. The thermal decomposition followed by *in situ* SR-PXD in combination with TG-DSC showed an amorphization of $KEr(BH_4)_4$ at ~170 °C. The decomposition of the post-annealed $KEr(BH_4)_4$ under high hydrogen pressure resulted in the formation of ErH_3 and KBH_4.

Acknowledgements

The research leading to these results has received funding from the People Program (Marie Curie Actions) of the European Union's Seventh Framework Program FP7/2007-2013/ under REA grant

agreement n° 607040 (Marie Curie ITN ECOSTORE) is thankfully acknowledged. The authors acknowledge the skillful assistance from the staff of the Swiss-Norwegian Beamlines (SNBL), at the European Synchrotron Radiation Facility (ESRF), Grenoble, France.

References

[1] Pillot, C., *The rechargeable battery market and main trends 2014-2015.* Avicenne Energy, 2015.

[2] Huot, J., ed. *Metal Hydrides*. Handbook of Hydrogen Storage, ed. M. Hirscher. 2010: Weinheim.

[3] Broom, D.P., *Hydrogen storage materials: the characterisation of their storage properties*. 2011: Springer Science & Business Media.

[4] Paskevicius, M., L.H. Jepsen, P. Schouwink, R. Černý, D.B. Ravnsbaek, Y. Filinchuk, M. Dornheim, F. Besenbacher, and T.R. Jensen, *Metal borohydrides and derivatives - synthesis, structure and properties.* Chemical Society Reviews, 2017. **46**(5): p. 1565-1634.

[5] Mohtadi, R. and S.-i. Orimo, *The renaissance of hydrides as energy materials.* Nature Reviews Materials, 2016. **2**: p. 16091.

[6] Sato, T., K. Miwa, Y. Nakamori, K. Ohoyama, H.-W. Li, T. Noritake, M. Aoki, S.-I. Towata, and S.-I. Orimo, *Experimental and computational studies on solvent-free rare-earth metal borohydrides R(BH4)3 (R= Y, Dy, and Gd).* Physical Review B, 2008. **77**(10): p. 104-114.

[7] Hagemann, H., M. Longhini, J.W. Kaminski, T.A. Wesolowski, R. Černý, N. Penin, M.H. Sørby, B.C. Hauback, G. Severa, and C.M. Jensen, *LiSc(BH4)4: a novel salt of Li+ and discrete Sc(BH4)4−complex anions.* The Journal of Physical Chemistry A, 2008. **112**(33): p. 7551-7555.

[8] Olsen, J.E., C. Frommen, M.H. Sørby, and B.C. Hauback, *Crystal structures and properties of solvent-free LiYb(BH4)4-xClx, Yb(BH4)3 and Yb(BH4)2-xClx.* Rsc Advances, 2013. **3**(27): p. 10764-10774.

[9] Jaroń, T. and W. Grochala, *Y(BH4)3—an old–new ternary hydrogen store aka learning from a multitude of failures.* Dalton Transactions, 2010. **39**(1): p. 160-166.

[10] Frommen, C., N. Aliouane, S. Deledda, J.E. Fonneløp, H. Grove, K. Lieutenant, I. Llamas-Jansa, S. Sartori, M.H. Sørby, and B.C. Hauback, *Crystal structure, polymorphism, and thermal properties of yttrium borohydride Y(BH4)3.* Journal of Alloys and Compounds, 2010. **496**(1): p. 710-716.

[11] Frommen, C., M.H. Sørby, P. Ravindran, P. Vajeeston, H. Fjellvåg, and B.C. Hauback, *Synthesis, crystal structure, and thermal properties of the first mixed-metal and anion-substituted rare earth borohydride LiCe(BH4)3Cl.* The Journal of Physical Chemistry C, 2011. **115**(47): p. 23591-23602.

[12] Ravnsbæk, D.B., Y. Filinchuk, R. Černý, M.B. Ley, D.r. Haase, H.J. Jakobsen, J.r. Skibsted, and T.R. Jensen, *Thermal polymorphism and decomposition of Y(BH4)3.* Inorganic chemistry, 2010. **49**(8): p. 3801-3809.

[13] Ley, M.B., L.H. Jepsen, Y.-S. Lee, Y.W. Cho, J.M.B. von Colbe, M. Dornheim, M. Rokni, J.O. Jensen, M. Sloth, and Y. Filinchuk, *Complex hydrides for hydrogen storage–new perspectives.* Materials Today, 2014. **17**(3): p. 122-128.

[14] Yan, Y., H.-W. Li, T. Sato, N. Umeda, K. Miwa, S.-i. Towata, and S.-i. Orimo, *Dehydriding and rehydriding properties of yttrium borohydride Y(BH4)3 prepared by liquid-phase synthesis.* International Journal of Hydrogen Energy, 2009. **34**(14): p. 5732-5736.

[15] Jaron, T., W. Kozminski, and W. Grochala, *Phase transition induced improvement in H2 desorption kinetics: the case of the high-temperature form of Y(BH4)3.* Physical Chemistry Chemical Physics, 2011. **13**(19): p. 8847-8851.

[16] Gennari, F.C. and M.R. Esquivel, *Synthesis and dehydriding process of crystalline Ce(BH4)3.* Journal of Alloys and Compounds, 2009. **485**(1–2): p. L47-L51.

[17] Li, H.-W., Y. Yan, S.-I. Orimo, A. Züttel, and C.M. Jensen, *Recent Progress in Metal Borohydrides for Hydrogen Storage.* Energies, 2011. **4**(1): p. 185-214.

[18] Zhang, B.J., B.H. Liu, and Z.P. Li, *Destabilization of LiBH4 by (Ce, La)(Cl, F)3 for hydrogen storage.* Journal of Alloys and Compounds, 2011. **509**(3): p. 751-757.

[19] Olsen, J.E., C. Frommen, T.R. Jensen, M.D. Riktor, M.H. Sørby, and B.C. Hauback, *Structure and thermal properties of composites with RE-borohydrides (RE= La, Ce, Pr, Nd, Sm, Eu, Gd, Tb, Er, Yb or Lu) and LiBH4.* RSC Advances, 2014. **4**(4): p. 1570-1582.

[20] Humphries, T.D., M.B. Ley, C. Frommen, K.T. Munroe, T.R. Jensen, and B.C. Hauback, *Crystal structure and in situ decomposition of Eu(BH4)2 and Sm(BH4)2.* Journal of Materials Chemistry A, 2015. **3**(2): p. 691-698.

[21] Černý, R., D.B. Ravnsbæk, G. Severa, Y. Filinchuk, V. D' Anna, H. Hagemann, D. Haase, J. Skibsted, C.M. Jensen, and T.R. Jensen, *Structure and Characterization of KSc(BH4)4.* The Journal of Physical Chemistry C, 2010. **114**(45): p. 19540-19549.

[22] Frommen, C., M. Heere, M.D. Riktor, M.H. Sørby, and B.C. Hauback, *Hydrogen storage properties of rare earth (RE) borohydrides (RE= La, Er) in composite mixtures with LiBH4 and LiH.* Journal of Alloys and Compounds, 2015. **645, Supplement 1**: p. S155-S159.

[23] Heere, M., S.H. Payandeh GharibDoust, C. Frommen, T.D. Humphries, M.B. Ley, M.H. Sørby, T.R. Jensen, and B.C. Hauback, *The influence of LiH on the rehydrogenation behavior of halide free rare earth (RE) borohydrides (RE= Pr, Er).* Physical Chemistry Chemical Physics, 2016. **18**(35): p. 24387-24395.

[24] Ley, M.B., M. Jørgensen, R. Černý, Y. Filinchuk, and T.R. Jensen, *From M(BH4)3 (M= La, Ce) Borohydride Frameworks to Controllable Synthesis of Porous Hydrides and Ion Conductors.* Inorganic Chemistry, 2016.

[25] Gennari, F., L.F. Albanesi, J. Puszkiel, and P.A. Larochette, *Reversible hydrogen storage from 6LiBH4–MCl3 (M= Ce, Gd) composites by in-situ formation of MH2.* International Journal of Hydrogen Energy, 2011. **36**(1): p. 563-570.

[26] Gennari, F.C., *Mechanochemical synthesis of erbium borohydride: Polymorphism, thermal decomposition and hydrogen storage.* Journal of Alloys and Compounds, 2013. **581**: p. 192-195.

[27] Ley, M.B., S. Boulineau, R. Janot, Y. Filinchuk, and T.R. Jensen, *New Li Ion Conductors and Solid State Hydrogen Storage Materials: LiM(BH4)3Cl, M= La, Gd.* The Journal of Physical Chemistry C, 2012. **116**(40): p. 21267-21276.

[28] Skripov, A.V., A.V. Soloninin, M.B. Ley, T.R. Jensen, and Y. Filinchuk, *Nuclear Magnetic Resonance Studies of BH4 Reorientations and Li Diffusion in LiLa(BH4)3Cl.* The Journal of Physical Chemistry C, 2013. **117**(29): p. 14965-14972.

[29] Ley, M.B., D.B. Ravnsbæk, Y. Filinchuk, Y.-S. Lee, R.l. Janot, Y.W. Cho, J. Skibsted, and T.R. Jensen, *LiCe(BH4)3Cl, a new lithium-ion conductor and hydrogen storage material with isolated tetranuclear anionic clusters.* Chemistry of Materials, 2012. **24**(9): p. 1654-1663.

[30] Roedern, E., Y.-S. Lee, M.B. Ley, K. Park, Y.W. Cho, J. Skibsted, and T.R. Jensen, *Solid state synthesis, structural characterization and ionic conductivity of bimetallic alkali-metal yttrium borohydrides MY(BH4)4 (M= Li and Na).* Journal of Materials Chemistry A, 2016. **4**(22): p. 8793-8802.

[31] Černý, R. and P. Schouwink, *The crystal chemistry of inorganic metal borohydrides and their relation to metal oxides.* Acta Crystallographica Section B: Structural Science, Crystal Engineering and Materials, 2015. **71**(6): p. 619-640.
[32] Marks, S., J.G. Heck, M.H. Habicht, P. Oña-Burgos, C. Feldmann, and P.W. Roesky, *[Ln(BH4)2(THF)2](Ln= Eu, Yb)□A Highly Luminescent Material. Synthesis, Properties, Reactivity, and NMR Studies.* Journal of the American Chemical Society, 2012. **134**(41): p. 16983-16986.
[33] Schouwink, P., E. Didelot, Y.-S. Lee, T. Mazet, and R. Černý, *Structural and magnetocaloric properties of novel gadolinium borohydrides.* Journal of Alloys and Compounds, 2016. **664**: p. 378-384.
[34] Schouwink, P., M.B. Ley, A. Tissot, H. Hagemann, T.R. Jensen, Ľ. Smrčok, and R. Černý, *Structure and properties of complex hydride perovskite materials.* Nature communications, 2014. **5**: p. 5706.
[35] Sato, T., K. Ikeda, M. Matsuo, K. Miwa, T. Otomo, S. Deledda, B.C. Hauback, G. Li, S. Takagi, and S.-i. Orimo, *In-situ powder neutron diffraction study on the formation process of LaMg2NiH7.* International Journal of Hydrogen Energy.
[36] Ley, M.B., M. Jørgensen, R. Černý, Y. Filinchuk, and T.R. Jensen, *From M(BH4)3 (M = La, Ce) borohydride frameworks to controllable synthesis.* 2016.
[37] Černý, R., G. Severa, D.B. Ravnsbæk, Y. Filinchuk, V. D'Anna, H. Hagemann, D. Haase, C.M. Jensen, and T.R. Jensen, *NaSc(BH4)4: a novel scandium-based borohydride.* The Journal of Physical Chemistry C, 2009. **114**(2): p. 1357-1364.
[38] Huang, L., O. Elkedim, and X. Li, *First principles investigation of scandium-based borohydride NaSc(BH4)4.* Journal of Alloys and Compounds, 2012. **536**: p. S546-S549.
[39] GharibDoust, S.P., M. Heere, M.H. Sørby, M.B. Ley, D.B. Ravnsbæk, B.C. Hauback, R. Černý, and T.R. Jensen, *Synthesis, structure and properties of new bimetallic sodium and potassium lanthanum borohydrides.* Dalton Transactions, 2016. **45**(47): p. 19002-19011.
[40] Brinks, H., A. Fossdal, R. Bowman, and B.C. Hauback, *Pressure–composition isotherms of TbNiAlHx.* Journal of Alloys and Compounds, 2006. **417**(1): p. 92-95.
[41] Hammersley, A., *FIT2D: An introduction and overview, ESRF Int.* Rep., ESRF97HA02T, 1997.
[42] Dyadkin, V., P. Pattison, V. Dmitriev, and D. Chernyshov, *A new multipurpose diffractometer PILATUS@SNBL.* Journal of Synchrotron Radiation, 2016. **23**(3): p. 825-829.
[43] Larson, A. and R. Von Dreele, *General Structure Analysis System (GSAS); Report LAUR 86-748; Los Alamos National Laboratory: Los Alamos, NM, 2000.* General Structure Analysis System (GSAS); Report LAUR 86-748; Los Alamos National Laboratory: Los Alamos, NM, 2000.
[44] Toby, B.H., *EXPGUI, a graphical user interface for GSAS.* Journal of applied crystallography, 2001. **34**(2): p. 210-213.
[45] Thompson, P., D. Cox, and J. Hastings, *Rietveld refinement of Debye–Scherrer synchrotron X-ray data from Al2O3.* Journal of Applied Crystallography, 1987. **20**(2): p. 79-83.
[46] Wegner, W., T. Jaroń, and W. Grochala, *Polymorphism and hydrogen discharge from holmium borohydride, Ho(BH4)3, and KHo(BH4)4.* International Journal of Hydrogen Energy, 2014. **39**(35): p. 20024-20030.
[47] Luck, R. and E. Schelter, *Potassium borohydride.* Acta Cryst. C, 1999. **55**.
[48] Paskevicius, M., M.B. Ley, D.A. Sheppard, T.R. Jensen, and C.E. Buckley, *Eutectic melting in metal borohydrides.* Physical Chemistry Chemical Physics, 2013. **15**(45): p. 19774-19789.
[49] Orimo, S., Y. Nakamori, and A. Züttel, *Material properties of MBH4 (M= Li, Na, andK).* Materials Science and Engineering: B, 2004. **108**(1): p. 51-53.

Supplement Information

for the manuscript

In situ investigations of bimetallic potassium erbium borohydride

Michael Heere[a], Seyed Hosein Payandeh GharibDoust[b], Magnus H. Sørby[a], Christoph Frommen[a], Torben R. Jensen[b] and Bjørn C. Hauback[a]

[a] Physics Department, Institute for Energy Technology, NO-2027 Kjeller, Norway

[b] Interdisciplinary Nanoscience Center (iNANO) and Department of Chemistry, University of Århus, Langelandsgade 140, DK-8000 Århus C, Denmark

Table A1 Atomic positions (x, y, z) and displacement factor (U_{iso}) of post-annealed $KEr(BH_4)_4$. Estimated standard deviations in brackets.

Atom	Postition	x	y	z	U_{iso}
K1	4*a*	0	0	0	0.039(14)
Er1	4*c*	0.5	0.132(1)	0.75	0.030(4)
B1	8*f*	0.5	0.252(12)	0.957(13)	0.034(49)
H1	8*f*	0.5	0.30(4)	0.06(5)	0.098(11)
H2	8*f*	0.5	0.17(5)	0.97(5)	0.098(11)
H3	16*h*	0.61(5)	0.26(3)	0.89(3)	0.098(11)
B2	8*g*	0.72(1)	0.01(1)	0.75	0.056(48)
H4	8*g*	0.84(5)	-0.03(5)	0.75	0.098(11)
H5	8*g*	0.75(7)	0.14(9)	0.75	0.098(11)
H6	16*h*	0.65(6)	-0.005(40)	0.85(4)	0.098(11)

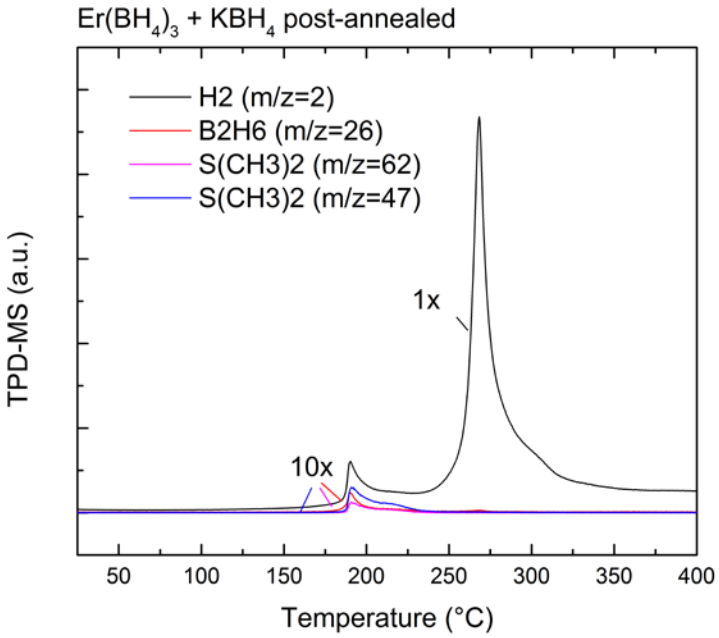

Fig. A1 TPD-MS of post-annealed $Er(BH_4)_3 + KBH_4$ heated from RT to 400 °C (heating rate 5 °C min^{-1}) showing release of H_2. The signal of $S(CH_3)_2$ and B_2H_6 has been multiplied by factor 10 for clarity reasons.

Fig. A2 TPPA pictures showing the white pellet consisting of $Er(BH_4)_4$ + KBH_4 (168 °C; far left), the onset of $KEr(BH_4)_4$ formation seen as a pink spot (177 °C), the pink color of the pellet after full conversion to $KEr(BH_4)_4$ (187 °C) and the dark pellet during different stages of the decomposition (240 °C and 264 °C). No melting is observed at any temperature up to 500 °C.